JOURNAL OF GEOPHYSICAL RESEARCH, VOL. 91, NO. B7, PAGES 7225–7239, JUNE 10, 1986

The 1977 Sumba Earthquake Series: Evidence for Slab Pull Force Acting at a Subduction Zone

WILLIAM SPENCE

U.S. Geological Survey, National Earthquake Information Center, Denver, Colorado

The great 1977 Sumba earthquake occurred at the eastern Sunda trench, just west of the collision of Australian continental lithosphere with the island arc. The length of the aftershock zone of this normal-faulting earthquake is about 200 km. Aftershocks are concentrated 65–115 km east of the main shock epicenter, with very few aftershocks in a 50-km-long segment that spans the main shock epicenter. Relocated hypocenters and focal mechanism data are consistent with normal faulting throughout the upper 28 km of the oceanic lithosphere. There is no evidence for thrust faulting of the deeper aftershocks. These data imply that the neutral bending surface must be at least 35–40 km deep. A second aftershock zone, about 180 km northwest of the main shock, became active immediately following the main shock, but events were concentrated during days 50–52. This zone is a 70-km-long lineation that trends toward the main shock epicenter and reflects right-lateral, strike-slip faulting within the subducted oceanic plate. Seismicity exists to a depth of about 650 km in the very old plate beneath the Sunda-Banda arc, and that plate's negative buoyancy causes very large slab pull forces. Great interface thrust earthquakes are absent at the Sumba region, and slab pull forces are inferred to have partially decoupled the subducted plate from the overriding plate. This decoupling permits slab pull stresses to be guided updip to the region of the Sumba main shock. Such shallow-acting slab pull provides a bending moment at the trench and explains the deformation and timing observed for the entire Sumba earthquake series. In this model, slab pull forces stretch the subducted plate until the increasing stresses at the shallow subduction zone lead to a subduction zone earthquake. Postseismically, the released oceanic plate undergoes a pulse of downdip strain, returning the plate to a less extended state. The moment of this downdip plate motion could exceed the seismic moment of the main shock.

INTRODUCTION

The great Sumba earthquake of August 19, 1977, is the largest normal-faulting earthquake (M_S 7.9, M_0 2.4–4.0 $\times 10^{28}$ dyn cm [*Given and Kanamori*, 1980; *Silver and Jordan*, 1983] to occur globally since the Sanriku earthquake of 1933. The Sumba earthquake occurred at the extreme eastern limb of the Sunda trench and south of Sumba Island. The main shock was followed by numerous normal-faulting aftershocks. Also following the main shock were right-lateral, strike-slip earthquakes at a location about 180 km northwest of the main shock [*Fitch et al.*, 1981; *Dziewonski et al.*, 1981]. The Sumba earthquake generated a large tsunami, causing wave heights in excess of 10 m on the coast of Sumbawa and 6 m on the north coast of Australia [*National Earthquake Information Service*, 1977].

Because earthquakes near oceanic trenches provide critical constraints on models of subduction zone processes, such earthquakes have been the subject of considerable recent research. Focal depths of trench, normal-faulting earthquakes often occur to 20 km into the lithosphere, whereas thrust-faulting earthquakes beneath trenches occasionally occur at depths over 40 km [*Forsyth*, 1982; *Ward*, 1983]. These data imply that the neutral bending surface often is 25–35 km deep [*Forsyth*, 1982], but the depth of the neutral surface can vary significantly from this range [*Ward*, 1983]. The bending indicated by such earthquakes is interpreted as a result of an oceanic plate moving into and through the zone of an oceanic trench [*Stauder*, 1968; *Spence*, 1977; *Chapple and Forsyth*, 1979; *Hanks*, 1979; *Imoto*, 1981; *Forsyth*, 1982; *Ward*, 1983]. The ridge push and slab pull forces are the primary forces causing plate movement. However, the possible relationship between these forces and plate bending has not been resolved.

Paper number 5B5447.

In rare instances, shallow thrust-faulting earthquakes occur near trenches [*Hanks*, 1971; *McAdoo et al.*, 1978; *Ward*, 1983; *Christensen and Ruff*, 1983]. These earthquakes are concentrated at the Kurile-Kamchatka region or are precursory to great, interface thrust earthquakes (e.g., prior to the 1985 Valparaiso earthquake [*Christensen and Ruff*, 1983, 1985; *Nishenko*, 1985]), and are explainable as being due to locally high compressional stresses.

The significant depths of great numbers of normal-faulting trench earthquakes jeopardize global models for the bending moment that require large horizontal compressional stresses [*Forsyth*, 1982] but favor models that require a vertically acting torque. Moreover, the shapes of trench and outer rise systems are best explained by a bending moment in the absence of large, horizontal stresses [*Caldwell et al.*, 1976; *Parsons and Molnar*, 1976; *Chapple and Forsyth*, 1979].

Thrust faulting earthquakes at a plate interface typically occur downdip from normal-faulting earthquakes near oceanic trenches. There is a historical absence of large interface thrust earthquakes downdip from the zone of the Sumba earthquake [*Cardwell and Isacks*, 1978; *McCann et al.*, 1979] and downdip from the immediate zone of the great (M_0 4.0 $\times 10^{28}$ dyn cm), normal-faulting 1933 Sanriku earthquake [*Kanamori*, 1971, 1972; *Mogi*, 1973]. Thus there is an anomalous lack of large interface thrust earthquakes directly downdip from the only known great and shallow, normal-faulting trench earthquakes. Because the 1977 Sumba earthquake is the largest recent normal-faulting earthquake near an oceanic trench, it provides an unusual opportunity to examine the nature of plate bending and the origin of bending stresses at oceanic trenches.

TECTONIC SETTING OF THE SUMBA EARTHQUAKE SERIES

The northward moving Australian continental lithosphere has been colliding with the Sunda-Banda arc for the last 3

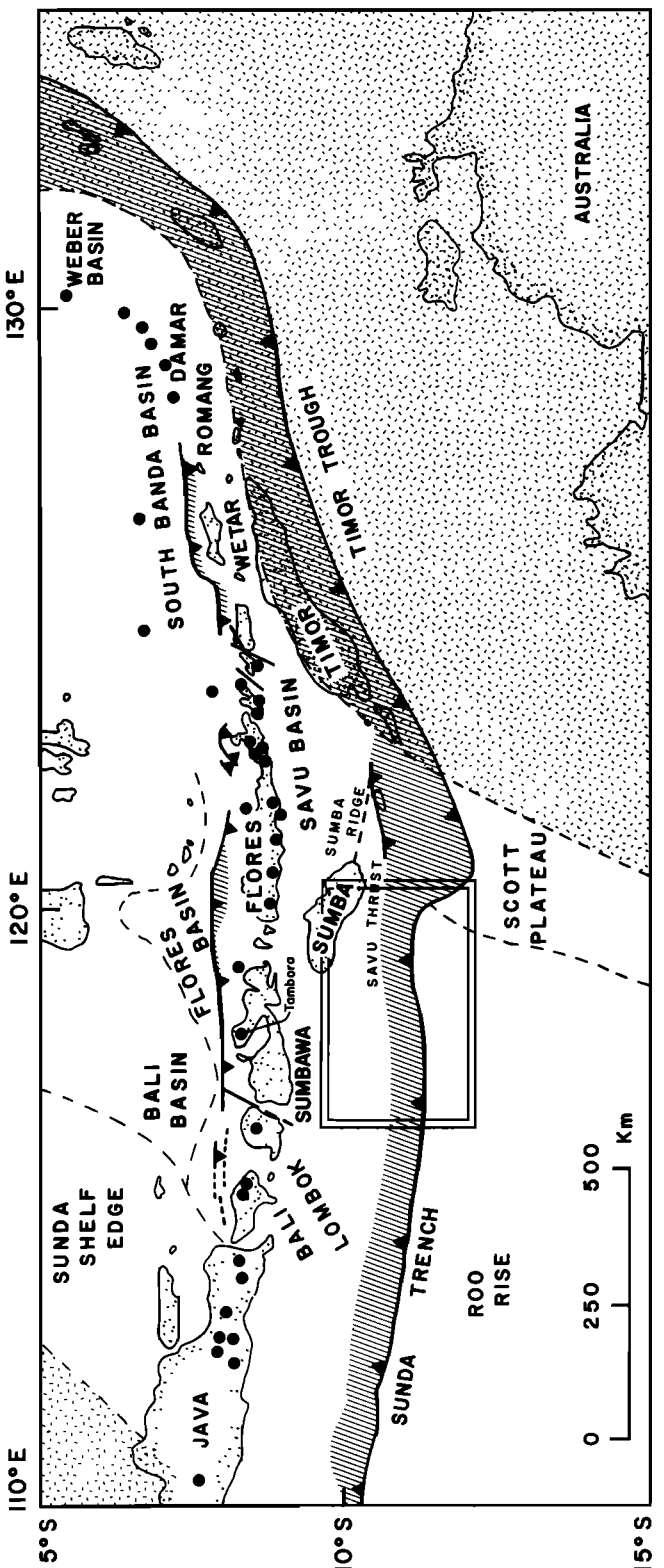

Fig. 1*a*. Regional setting of the 1977 Sumba earthquake series (study area shown by inset). Major tectonic features in the central Sunda-Banda arc. Locations shown for active volcanoes [from *Simkin et al.*, 1981], major thrusts, accretionary wedges, and extent of continental crust (modified from *Hamilton* [1979] and *Silver et al.* [1983]).

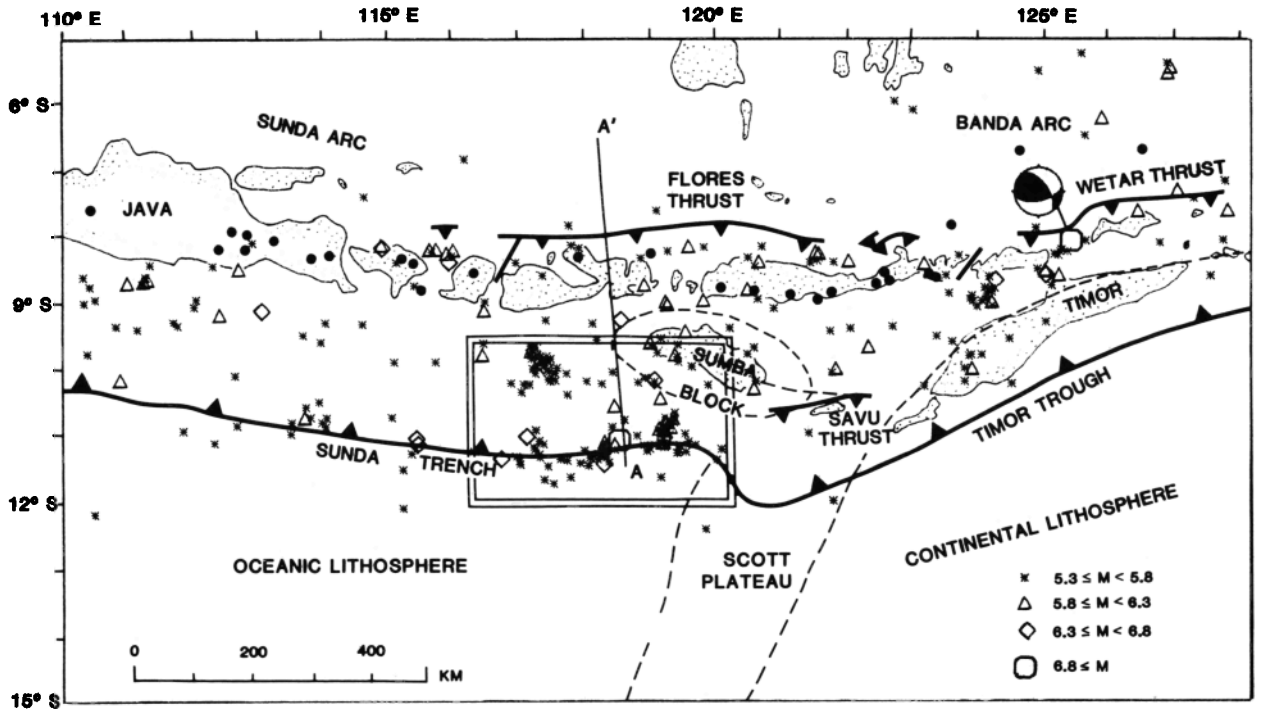

Fig. 1*b*. Shallow seismicity ($h < 100$ km) for the period 1963–1984 and for $m_b \geq 5.3$. This plot includes the 1977 Sumba earthquake series (study area shown by inset) and shows a focal mechanism solution of the M_S 6.8 Timor earthquake of August 27, 1977, near the Wetar thrust. Compare lack of seismicity at the Timor trough with active seismicity at the Sunda trench. Volcanoes, major thrusts, and extent of continental crust as shown in Figure 1*a*.

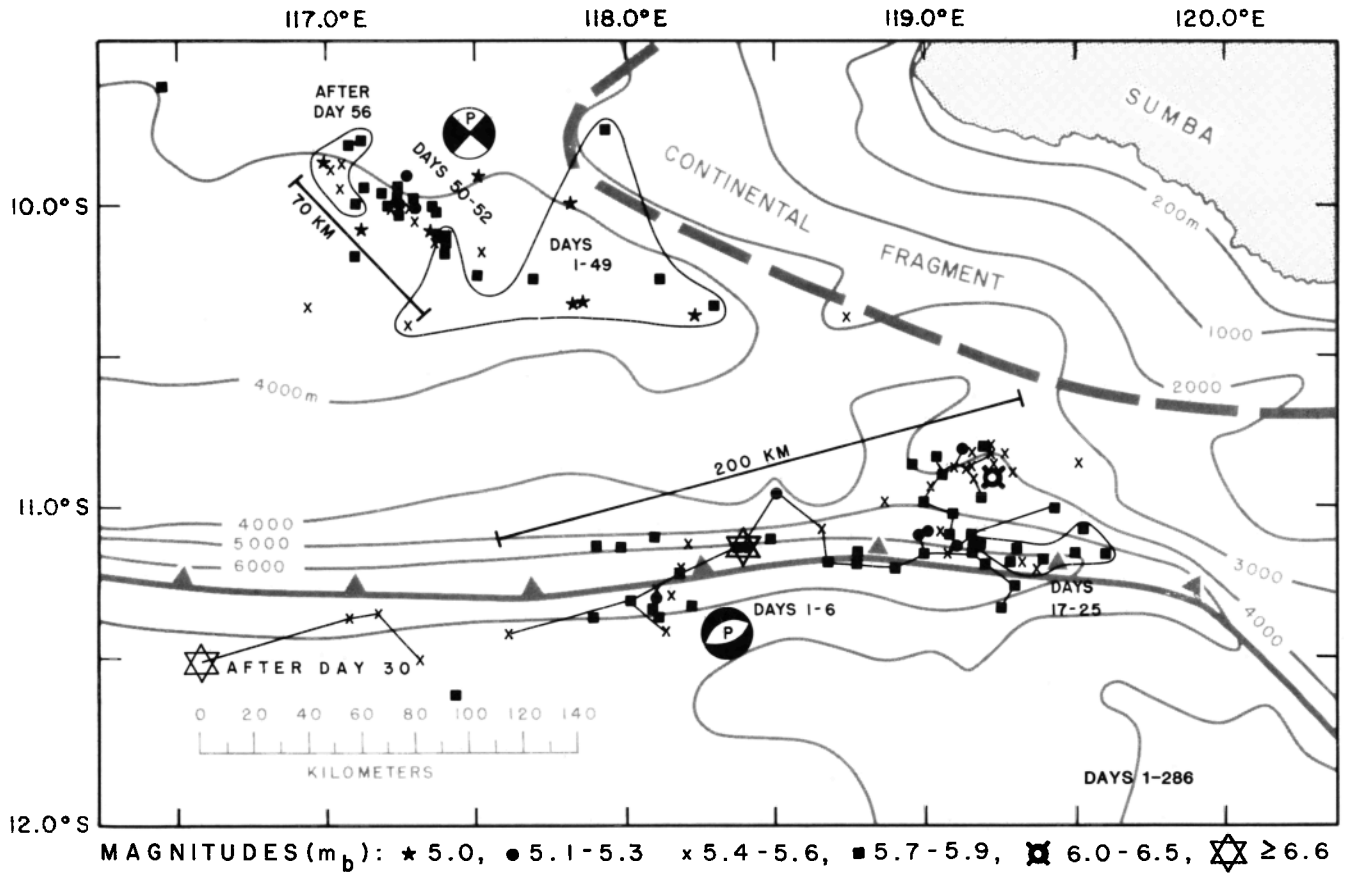

Fig. 2. The two groups of epicenters that comprise the 1977 Sumba earthquake series, based on JHD hypocenter relocations. Main shock shown by heavy lined star. Days 1–6 of activity at the trench zone shown by lines connecting epicenters; later space-time groupings of epicenters also indicated. Typical focal mechanisms shown for each group. Bathymmetry, axis of eastern Sunda trench, and position of Sumba continental fragment from *Hamilton* [1979].

m.y. [*Katili*, 1975; *Hamilton*, 1979; *Bowin et al.*, 1980; *Johnston and Bowin*, 1981; *Silver et al.*, 1983]. The collision zone now extends eastward from about 120°E and comprises the Banda portion of the Sunda-Banda arc (Figure 1). At the zone of the continental-arc collision there is no oceanic plate to be cycled through the former trench zone, and conventional subduction cannot be occuring there. However, conventional subduction occurs west of about 110°E, as both interface thrust-faulting and trench normal-faulting earthquakes occur with the subduction of oceanic lithosphere [*Cardwell and Isacks*, 1978; *Fitch and Molnar*, 1970; *Fitch*, 1970, 1972]. Therefore the zone of the eastern Sunda arc, between about 115°E and 120°E, is a transition region between typical subduction at the central Sunda arc and modified subduction at the western Banda arc. The 1977 Sumba main shock occurred at this transition region.

Given a convergence rate of 78 km/m.y. [*Weissel and Hayes*, 1974; *Vogt et al.*, 1983], for the continental-arc collision of the last 3 m.y. implies that we should see evidence of about 230 km of lithospheric shortening between Australia and the Banda arc. About 30 km of this shortening has resulted from back arc thrusting, in progress in the South Banda and Flores basins [*Hamilton*, 1979; *Silver et al.*, 1983]. *Bowin et al.* [1980] and *Johnston and Bowin* [1981] argue that the remainder of compression at this tectonic front has been taken up by thickening and uplift of the outer arc ridge, but *McCaffrey et al.* [1985] show that these processes are insufficient to accommodate nearly 200 km of lithospheric shortening.

Seismic reflection and refraction studies show that the Australian continental lithosphere is continuous through the outer Banda arc [*Curray et al.*, 1977; *Hamilton*, 1979], and this lithosphere is deduced to have thrust beneath Timor [*Chamalaun and Grady*, 1978; *Hamilton*, 1979; *Bowin et al.*, 1980; *McCaffrey et al.*, 1985]. Subduction of continental lithosphere to depths of 100–150 km [*McCaffrey et al.*, 1985] possibly has occurred. Such subduction is consistent with the lack of lithospheric shortening and lack of indentation at the western Banda arc. The possibility of limited subduction of continental lithosphere previously has been considered by *Molnar and Gray* [1979], *Roecker* [1982], and *Pennington* [1984].

Bowin et al. [1980] and *Johnston and Bowin* [1981] found that over the last 2 m.y. the relative motion at the Timor trough between the Australian lithosphere and the western Banda arc has slowed to nearly zero. Thus subduction of Australian continental lithosphere nearly has stopped. Simultaneously, however, the northward velocity of Australia has not slowed [*Weissel and Hayes*, 1974; *Vogt et al.*, 1983] and the development of back arc thrusts reflects the resulting compression. Yet the shallow 1977 Sumba earthquake occurred near this zone of compression, and the origin of the large tensional stresses causing the Sumba earthquake requires explanation.

RELOCATION OF HYPOCENTERS

To interpret better the 1977 Sumba earthquake series and because catalog hypocenters are suspect, the method of joint hypocenter determination (JHD) was used to relocate the teleseismically recorded Sumba earthquakes. Data from earthquake catalogs of the U.S. Geological Survey and the International Seismological Centre (ISC) show focal depths for these earthquakes predominantly to be 33 km for the Sunda trench zone and 0 km for the secondary zone. The ISC catalog indicates focal depths for three aftershocks to be greater than 70 km. The depths of 33 km and 0 km usually are default values that are assigned to shallow earthquakes when the computed depth is above sea level. This difficulty arises from a lack of depth phases, lack of nearby seismographic stations, and use of a velocity model that is inappropriate for the region of interest.

By modeling depth phases from long-period P wave signals, *Fitch et al.* [1981] determined focal depths for five aftershocks near the trench, finding four of them to be within 15 km of the seafloor and the other at a depth of 24 km. Although *Dziewonski et al.* [1981] determined moment tensors for the larger Sumba aftershocks, they did not publish the corresponding focal depths. In the present study, redetermination of focal depths was emphasized because of the implications that these focal depths have on the nature of rupture of the main shock and the nature of plate bending at the Sumba earthquake zone. Data for depth phases were read from World-Wide Standard Seismograph Network (WWSSN) stations for many earthquakes in Figures 2 and 3. This complete suite of the larger Sumba aftershocks should directly reflect the primary tectonic processes of this unusual earthquake series.

For the time interval May 1, 1977, to May 31, 1978, the relevant arrival time data were obtained from the ISC catalog for the zone 9.0°–12.5°S × 116.0°–120.°E and combined with depth phase data read for this study. The earthquakes to be relocated were divided into two main groups because the main shock and primary aftershock series occurred in and near the Sunda trench, whereas the secondary aftershock series occurred 90–220 km north and northwest of the main sequence and on the west side of the Sumba continental fragment. Fifteen well-recorded earthquakes were selected from each group of aftershocks. The earthquakes from each of these sets were relocated by the JHD method [*Dewey*, 1971; *Dewey and Spence*, 1979], and the resulting data were used to estimate the station adjustments, variances, and phase weightings of the seismic phases P, S, pP, and PKP at each station. These JHD-computed station adjustments and variances were then used in a single event location method to determine the locations given in Figures 2 and 3. The precision of a redetermined hypocenter is estimated from 90% confidence ellipses on the three hypocentral coordinate pairs. Seventy-nine earthquakes of $m_b \geq 5.1$ were relocated in the zone of the Sunda trench and 45 earthquakes of $m_b \geq 5.0$ were relocated in the secondary aftershock zone.

As a check on JHD depths over 40 km below sea level, digital data from Seismic Research Observatory (SRO) stations were examined for four of the deepest aftershocks near the Sunda trench. Figure 4 shows waveforms for two of these earthquakes. The depth phases pP, sP, and swP are exceptionally clear. The pwP phase is obscured in the coda of the sP phase. The sP phase shows the longer period expected for that phase, and the swP phase shows the ringing that is characteristic of water phases. For KAAO, $pwP\text{-}pP \approx swP\text{-}sP \approx 5.3$ s, and for CHTO these intervals ≈ 7.3 s. The depth phases for the earthquakes of September 16 at 0630 and September 5 at 1117 indicate focal depths of 26 km and 28 km beneath the seafloor (or 32 and 34 km below sea level). Similarly determined focal depths for the aftershocks of August 19 at 1528 and August 19 at 2051 are 25 km and 28 km beneath the seafloor. The focal depths of these four deep aftershocks are about 10 km shallower than the corresponding JHD depths. It is concluded that the deepest aftershocks of the 1977 Sumba earthquake are about 28 km beneath the seafloor.

The P wave first motions of the deep aftershocks are dilatational. In the context of a plate being bent at the Sunda

a. SUNDA TRENCH ZONE

OCCURRENCE TIME (GMT)	DAY	Φ °S	λ °E	h km	m_b	CONFIDENCE EPI-CENTER km	CONFIDENCE DEPTH km	OCCURRENCE TIME (GMT)	DAY	Φ °S	λ °E	h km	m_b	CONFIDENCE EPI-CENTER km	CONFIDENCE DEPTH km
77 819 5 8	1	-11.13	118.41	(31)	5.8	7	20	77 825 18 9	7	-10.97	118.86	10	5.6	51	55
77 819 6 8	1	-11.11	118.39	(27)	6.8	7	18	77 825 19 8	7	-10.81	119.26	12	5.4	12	35
77 819 643	1	-10.95	118.50	63	5.9	20	35	77 825 2140	7	-10.88	119.29	27	5.4	12	29
77 819 7 4	1	-11.00	119.43	53	5.1	21	37	77 826 141	8	-11.36	117.89	29	5.2	13	26
77 819 714	1	-10.83	119.03	58	5.3	27	44	77 826 826	8	-10.85	119.23	(20)	5.5	7	12
77 819 1050	1	-10.96	119.18	19	5.3	16	47	77 827 1727	9	-11.13	118.38	17	5.1	13	29
77 819 1133	1	-11.06	118.65	0	5.4	11	41	77 830 2110	12	-11.07	119.05	10	5.4	10	30
77 819 1323	1	-10.86	119.09	(31)	5.6	7	21	77 9 1 1125	14	-11.13	117.90	34	5.1	14	29
77 819 1332	1	-11.33	119.25	0	5.1	36	95	77 9 1 1313	14	-11.63	117.44	1	5.3	10	32
77 819 1528	1	-11.22	118.18	46	5.3	12	17	77 9 1 1351	14	-11.15	118.77	14	5.1	12	11
77 819 1740	1	-11.31	118.01	39	5.2	11	26	77 9 2 1036	15	-11.08	119.01	(7)	5.8	7	23
77 819 1938	1	-10.80	119.12	(11)	5.8	8	25	77 9 2 1343	15	-10.84	119.51	53	5.4	22	22
77 819 2020	1	-10.90	119.16	20	5.6	7	8	77 9 4 344	17	-11.15	119.50	23	5.1	11	24
77 819 2051	1	-11.18	118.77	44	5.2	10	14	77 9 5 249	18	-11.15	119.15	0	5.2	67	80
77 819 2135	1	-10.86	119.14	20	5.5	7	9	77 9 5 1117	18	-11.11	118.21	40	5.5	9	14
77 820 358	2	-10.92	119.02	32	5.6	13	36	77 9 6 1713	19	-11.15	119.60	27	5.3	12	28
77 820 420	2	-11.20	118.18	0	5.5	8	27	77 9 7 119	20	-11.08	119.52	(25)	5.3	10	24
77 820 712	2	-11.02	119.09	22	5.1	16	14	77 913 1330	26	-11.17	119.39	16	5.2	9	23
77 820 921	2	-11.13	119.10	(32)	5.7	7	12	77 915 1348	28	-11.18	119.28	0	5.1	11	10
77 820 1117	2	-11.09	119.08	5	5.1	12	33	77 916 630	29	-11.13	117.98	45	5.3	9	13
77 820 1236	2	-11.09	119.15	36	5.2	22	52	77 923 557	36	-11.31	118.10	(14)	5.8	7	7
77 820 1916	2	-11.09	118.98	(0)	5.9	8	7	77 925 1831	38	-11.35	117.18	(18)	5.4	9	22
77 820 1944	2	-10.82	119.22	34	5.4	20	49	77 929 216	42	-11.32	118.21	29	5.3	11	24
77 821 212	3	-11.20	118.90	23	5.3	8	21	7710 5 18 4	48	-11.50	117.31	27	5.4	9	24
77 821 221	3	-11.16	119.00	21	5.3	12	15	7710 5 1851	48	-11.36	117.08	0	5.5	8	29
77 821 650	3	-11.19	118.68	20	5.2	13	30	7710 7 1438	50	-11.17	119.32	19	5.4	9	31
77 821 751	3	-11.12	119.17	32	5.1	11	26	7710 7 1520	50	-11.14	119.30	21	5.1	12	29
77 821 929	3	-11.25	119.29	9	5.2	10	29	771012 122	55	-11.21	119.36	17	5.6	8	23
77 821 1039	3	-10.98	118.99	15	5.1	10	25	771016 146	59	-11.36	118.11	1	5.1	11	37
77 821 1536	3	-11.15	119.07	11	5.6	8	27	7712 3 1250	107	-11.34	118.09	38	5.3	18	57
77 821 2029	3	-10.79	119.22	26	5.4	10	25	7712 6 1752	110	-11.29	118.15	10	5.5	8	12
77 821 2037	3	-10.89	119.05	16	5.3	13	26	78 310 1358	204	-10.80	119.19	7	5.3	13	43
77 823 1024	5	-11.41	117.61	21	5.5	8	12	78 310 1725	204	-10.86	119.14	22	5.4	13	32
77 823 1542	5	-11.18	119.20	0	5.1	18	17	78 310 18 1	204	-10.81	119.15	26	5.2	19	52
77 823 23 6	5	-11.41	118.13	14	5.4	11	32	78 311 1154	205	-10.81	119.15	14	5.4	11	32
77 824 942	6	-11.27	118.10	46	5.5	13	15	78 327 8 5	221	-11.10	118.48	35	5.2	15	40
77 824 2217	6	-11.09	118.09	43	5.1	15	18	78 410 2052	235	-11.50	116.58	(0)	6.6	8	26
77 825 18 5	7	-10.90	119.23	(18)	6.0	7	20	78 422 1955	247	-10.85	118.95	7	5.1	14	60

b. SECONDARY ZONE

77 819 738	1	-10.39	117.28	28	5.4	20	62	7710 7 2136	50	-9.98	117.25	(11)	5.7	8	28
77 824 2 8	6	-10.32	117.82	28	5.0	14	34	7710 7 2247	50	-10.03	117.24	29	5.1	12	31
77 824 19 0	6	-10.32	117.85	35	5.0	13	30	7710 7 2323	50	-10.17	117.09	27	5.3	18	35
77 825 2311	7	-10.33	118.29	(28)	5.3	10	28	7710 8 158	51	-10.08	117.11	4	5.0	11	37
77 829 952	11	-10.36	118.22	23	5.0	13	34	7710 8 1052	51	-10.00	117.21	39	5.2	10	26
77 9 3 1333	16	-9.99	117.81	50	5.0	15	22	7710 8 18 8	51	-9.98	117.29	21	5.2	9	8
77 9 6 2159	19	-9.74	117.93	52	5.1	18	21	7710 8 1859	51	-10.09	117.36	38	5.0	12	32
77 915 1113	28	-10.10	117.40	50	5.1	14	17	7710 8 1930	51	-10.08	117.35	31	5.0	12	33
77 916 440	29	-10.24	118.11	(39)	5.3	10	29	7710 9 10 3	52	-9.95	117.18	39	5.3	9	26
77 916 1222	29	-10.24	117.69	40	5.2	9	16	7710 9 1657	52	-10.12	117.36	22	5.4	11	11
7710 1 1252	44	-10.12	117.40	(17)	5.3	8	22	771016 21 9	59	-9.87	117.01	(21)	5.5	8	23
7710 1 20 2	44	-10.16	117.39	38	5.2	9	25	771016 2122	59	-9.78	117.11	48	5.3	10	18
7710 7 445	50	-10.04	117.29	(20)	5.6	7	7	771016 2313	59	-9.90	117.50	44	5.0	20	25
7710 7 539	50	-10.15	117.52	22	5.4	9	8	771017 953	60	-9.85	116.99	29	5.0	16	34
7710 7 830	50	-10.02	117.36	23	5.1	10	28	771020 1135	63	-9.79	117.07	18	5.2	9	8
7710 7 1210	50	-10.00	117.29	(14)	5.9	7	7	771025 650	68	-9.85	117.05	17	5.4	9	8
7710 7 1223	50	-9.99	117.35	132	5.1	20	43	771030 150	73	-10.36	118.73	9	5.6	9	38
7710 7 1650	50	-9.98	117.24	30	5.1	12	32	771031 1139	74	-10.23	117.50	45	5.1	12	19
7710 7 17 1	50	-9.99	117.28	(27)	5.6	8	24	78 225 610	201	-9.93	117.05	15	5.6	9	9
7710 7 1736	50	-9.89	117.26	(21)	5.7	7	7	78 225 1412	201	-9.99	117.10	29	5.1	11	29
7710 7 1758	50	-9.94	117.12	0	5.1	17	15	78 315 1446	209	-9.60	116.45	83	5.2	10	14
7710 7 19 4	50	-10.01	117.22	23	5.5	8	25	78 5 4 1811	259	-10.32	116.93	23	5.4	11	28
7710 7 1910	50	-9.94	117.24	25	5.3	10	10								

Fig. 3. JHD relocated hypocenters for (*a*) the 79 earthquakes $m_b \geq 5.1$ for the zone of the Sunda trench and (*b*) the 45 earthquakes $m_b \geq 5.0$ in the secondary zone. Events with encircled depths are those for which focal mechanism solutions are given. Depths are given below sea level. Last two columns are derived from projections of the 90% hypocentral confidence ellipses and are respectively the length of semimajor axis of the epicentral confidence ellipse and the largest of the semimajor axes of depth with latitude and of depth with longitude.

trench, these data are consistent with normal faulting above a neutral bending surface. The depths of these normal-faulting aftershocks are deeper than but in general agreement with results for other trench zones in the circum-Pacific region [*Chapple and Forsyth*, 1979; *Forsyth*, 1982; *Ward*, 1983]. Following *Chapple and Forsyth* [1979], these normal-faulting aftershocks imply the depth of the neutral bending surface to be at least 35–40 km below the seafloor.

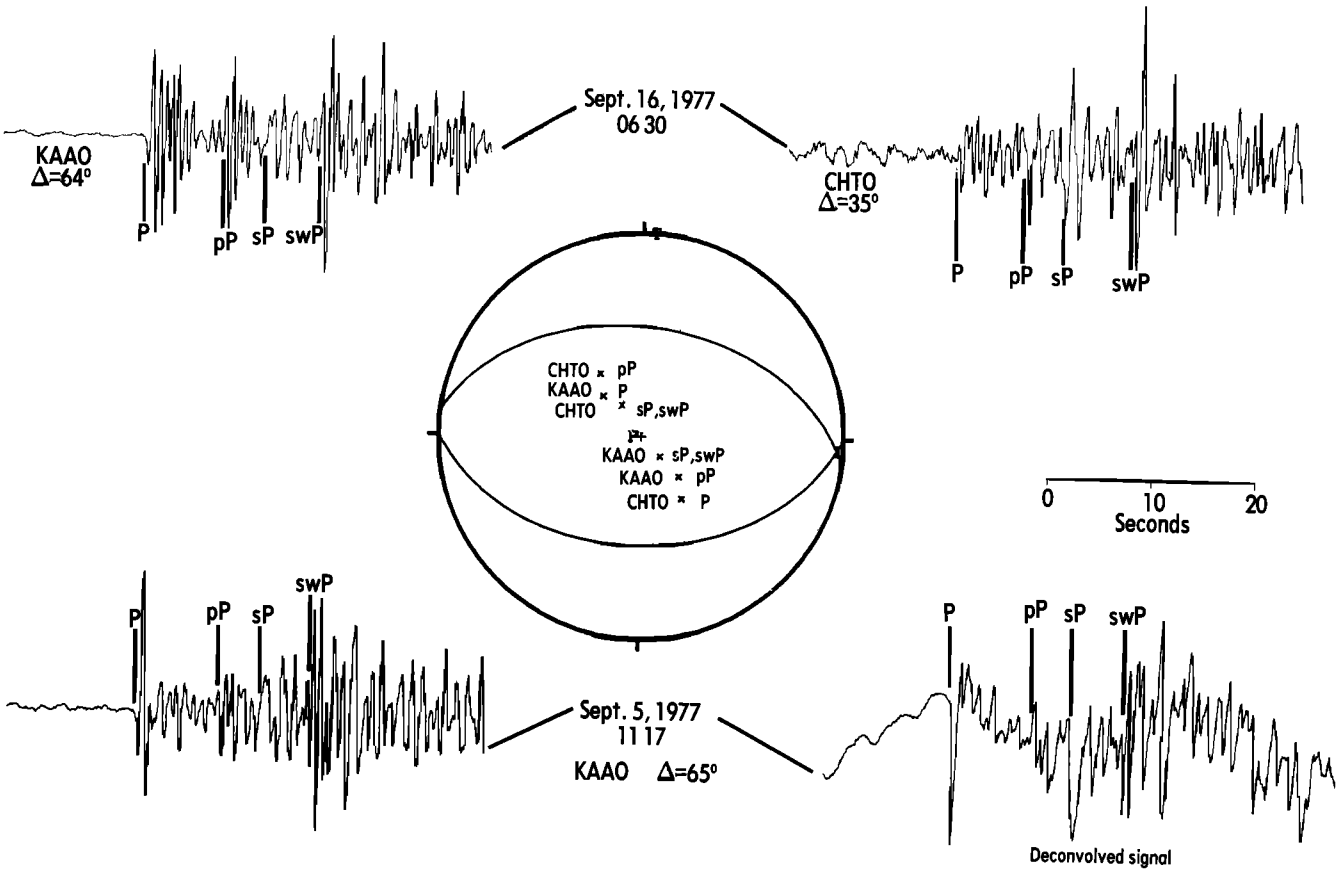

Fig. 4. Waveforms for two of the deepest aftershocks (September 16, h = 32 km and September 5, h = 34 km), showing depth phases *pP*, *sP*, and *swP* recorded at SRO stations. Angles of incidence at the stations KAAO and CHTO are shown on the lower focal hemisphere for phases *P*, *pP*, *sP*, and *swP*. Waveform signal at lower right is the deconvolved signal of the SRO short-period signal shown at lower left. The deconvolved signal is broadband and eliminates instrument resonance at 1 Hz, thus better representing the signal leaving the source than the signal passed through the instrument.

A vertical section of all relocated hypocenters is shown by pluses in Figure 5. This vertical section, striking N5°W, overlays a similar section of hypocenters from the ISC catalog for the time interval 1963–1976 for the region 6.0°–12.5°S × 108.0°–122.0°E. The zero point on the abscissa is the epicenter of the Sumba main shock. The upper surface of the shallow-dipping (7°N) subducted oceanic lithosphere is taken from profile 9A of *Hamilton* [1979]. Depths of foci computed in this study indicate that events in the secondary aftershock zone are within the oceanic lithosphere rather than in the overriding plate. A sudden increase in dip of the subducting oceanic lithosphere occurs at a depth of about 30 km. This slab bend is apparent in Figure 5 where the downdip extrapolation of the known position of the shallow subducting oceanic plate is met by the intermediate depth seismicity which follows a smooth 45° dipping trend. The northernmost aftershocks of the secondary zone tend to be within and downdip of this slab bend.

Space-Time Development of the Aftershock Series

The only foreshock in this data set occurred 1 hour prior to and spatially very close to the main shock. In the zone of the Sunda trench, 58 of the 79 events (73%) occurred by day 20 and 66 events (84%) occurred by day 50. Although the first aftershock in the secondary zone occurred 1.5 hours after the main shock, only 12 of the 45 events (27%) in this zone occurred prior to day 50 of the aftershock series; 21 events (47%) occurred during a 60-hour period of days 50–52. Aftershocks for days 1–49, with focal mechanism solutions for the larger events, are shown in Figure 6*a*, and aftershocks for days 50–286, with focal mechanisms for the larger events, are shown in Figure 6*b*.

Main Zone

Aftershocks during the first 4 days occurred throughout a 200-km-long zone but primarily 30–120 km east and 20–50 km west of the main shock (Figure 2). The greatest aftershock concentration was 65–115 km east of the main shock. Very few aftershocks occurred in a 50-km-long zone spanning the main shock; this quiet zone is included in the 80-km-long zone inferred as the primary rupture for the main shock [*Lynnes et al.*, 1985]. Following the first month, a small group of earthquakes, including the M_S 6.6 event of April 10, 1978, extended the active trench zone 120 km farther westward. This distribution of aftershocks may indicate that following the main shock, very little residual stress remained near the main shock.

The easternmost Sunda trench aftershocks are near the western edge of the Scott Plateau (Figure 1*b*), which is in thrust contact with the forearc accretionary wedge [*Silver et al.*, 1983]. *Stagg* [1978] inferred that the crust of the Scott Plateau is 23–24 km thick. Because the crust of the Scott plateau is much thicker than the crust of the adjoining oceanic

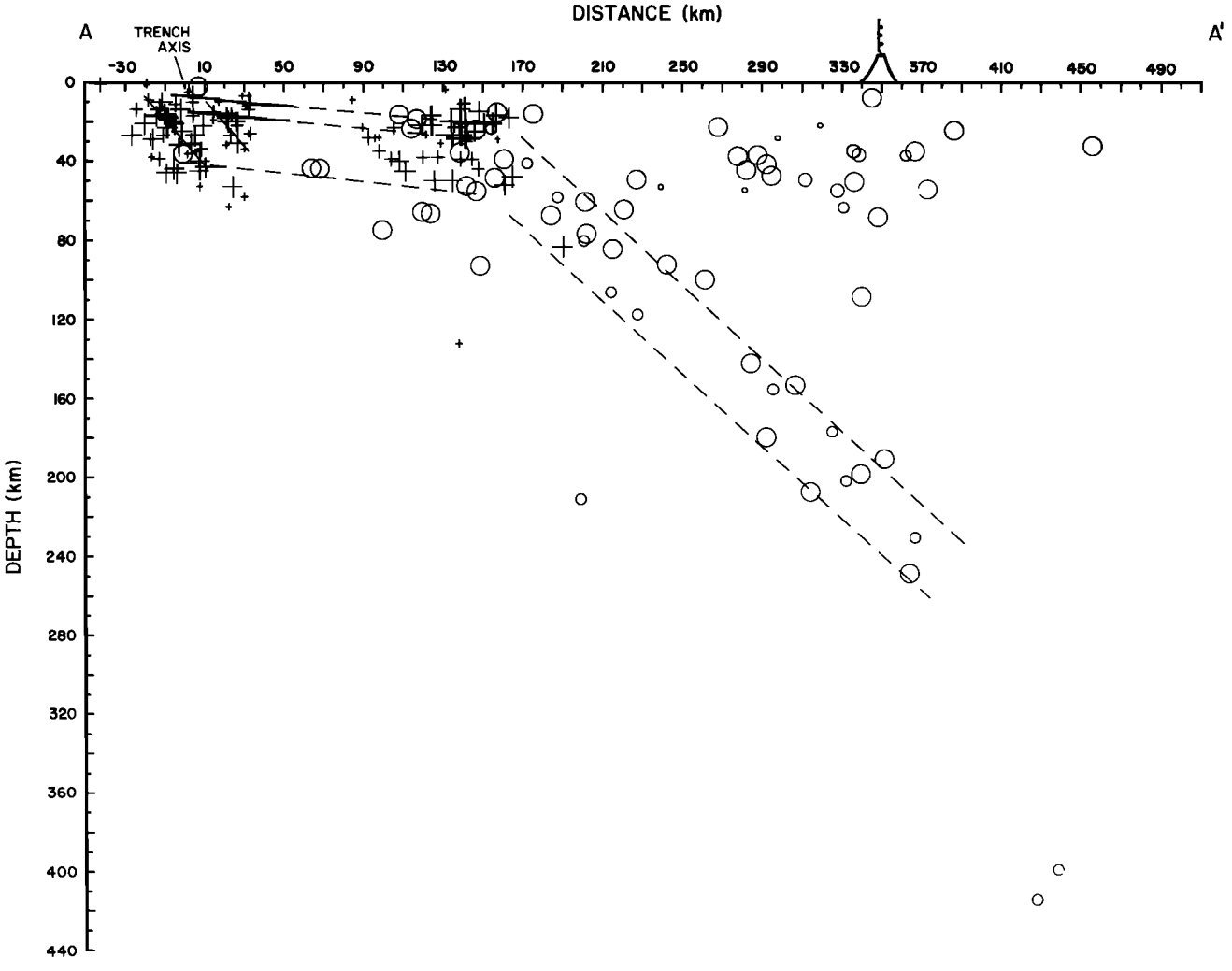

Fig. 5. Vertical section of hypocenters of Figure 2, shown by pluses superimposed on vertical section of ISC hypocenters, 1963–1976, for the region 6.0°–12.5°S × 108.0°–122.0°E, and for $m_b \geq 5.3$, shown by circles. For each data set there are three symbol sizes: largest symbol represents hypocenter based on greater than 110 *P* wave observations, intermediate-sized symbol represents hypocenter based on 60–110 *P* wave observations, and smallest symbol represents hypocenter based on less than 60 *P* wave observations. Sections taken along line A-A', through the Sumba main shock and perpendicular to the local trench axis, are shown in Figure 1*b*. Hypothetical fault planes that dip 45°N are drawn through the two hypocentral groups near the Sunda trench. Oceanic crust (solid lines) dips 7°N [*Hamilton*, 1979] and is extrapolated (dashed lines) to zone where ISC hypocenters suggest a sudden increase in dip. Thickness of brittle part of this 148-m.y.-old lithosphere is taken as about 35 km [*Watts et al.*, 1980]. This figure indicates that both the Sunda trench aftershock groups and the aftershock group west of the Sumba continental fragment occur within the subducting oceanic lithosphere.

lithosphere and if this plateau has subducted beneath the trench, then the Scott Plateau could act as a rupture barrier at the eastern side of the Sumba earthquake series. Although the easternmost aftershocks have stress drops only of the order of 10 bars [*Fitch et al.*, 1981] this concentration of aftershocks probably reflects stress adjustments due to incomplete rupture by the main shock.

Secondary Zone

Prior to day 50, there occurred strike-slip aftershocks throughout a large sector east of the northwest trending lineation but west of the Sumba continental fragment (Figure 6*a*). Secondary zone aftershocks were concentrated during days 50–52 in a 30-km-long, northwest trend located about 180 km from the main shock. During the first 17 hours of day 50 (October 7, 1977), there were seven earthquakes of $m_b \geq 5.5$ in this small segment. The secondary zone was active before and after days 50–52, giving it a total length of about 70 km (Figure 6). Focal mechanisms for earthquakes in the lineation are consistent with right-lateral, vertical strike-slip faulting along the trend of earthquakes. These earthquakes are within the subducting oceanic lithosphere just west of the thick Sumba continental fragment. A line were fitted through these earthquakes, at the azimuth of the typical fault plane, trends directly to the main shock epicenter (Figure 2).

FOCAL MECHANISMS

Most focal mechanism solutions shown in Figure 6 are the conditioned Rayleigh wave solutions of *Fitch et al.* [1981] obtained from use of SRO and Abbreviated SRO (ASRO) data. Focal depths recomputed by the JHD method show that the large aftershocks having focal mechanisms are at relatively shallow depths (Figure 3), whereas smaller but well-located aftershocks occur to depths of 28 km into the lithosphere. The

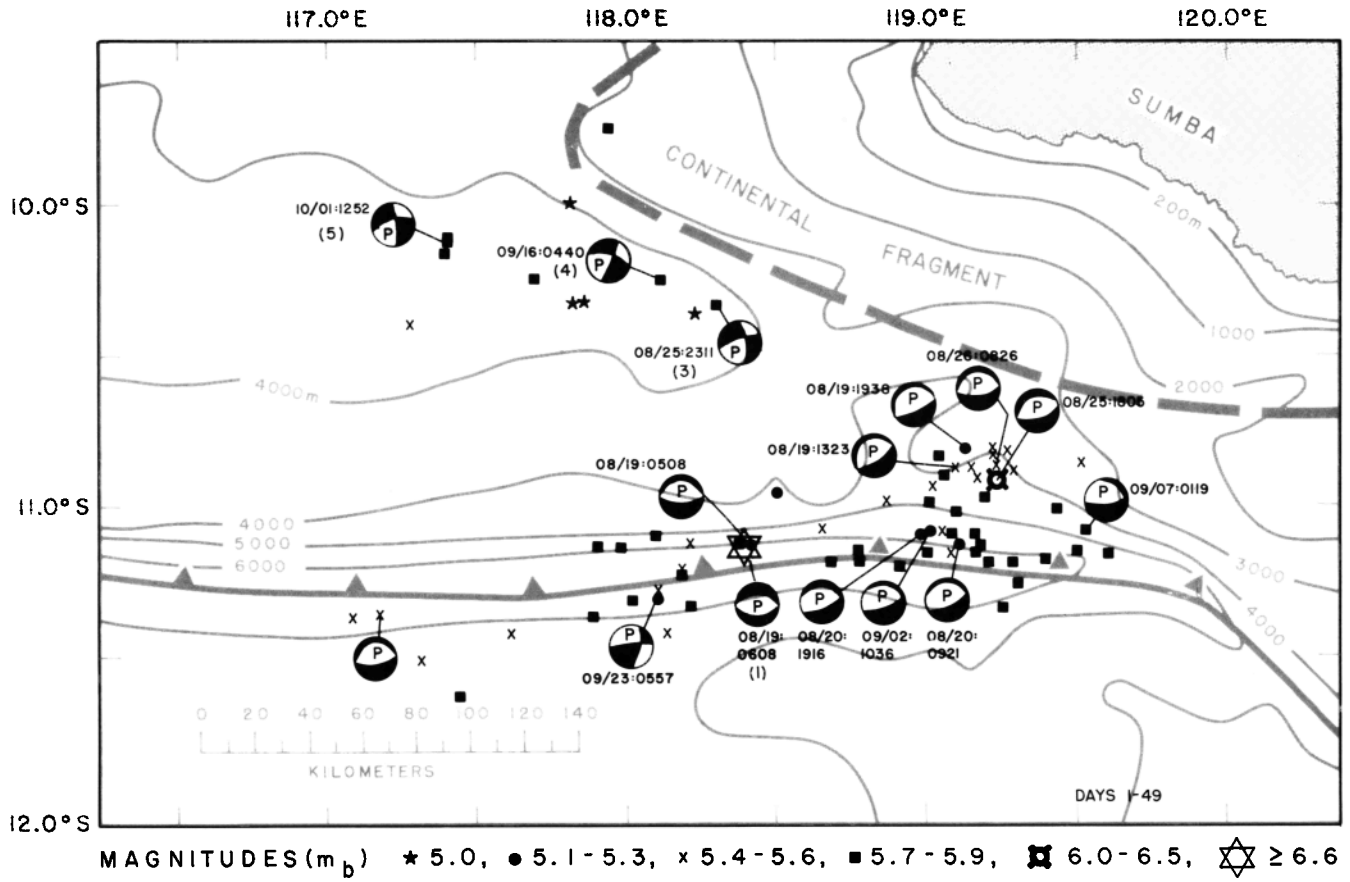

Fig. 6*a*

Fig. 6. (a) Main shock and aftershock locations with associated focal mechanism solutions for events occurring before day 50. (b) Aftershock locations with associated focal mechanism solutions for events occurring during days 50–286. For these figures, shaded quadrants indicate regions of compressional *P* wave first motions. Numbers in parentheses indicate focal mechanisms done in this study, shown in detail in Figure 7 and described in Table 1. Unnumbered focal mechanisms refer to those of *Fitch et al.* [1981]. See text.

focal mechanisms for aftershocks in and near the Sunda trench indicate normal faulting, with a very shallow north dipping plane and a very steep south dipping plane [*Fitch et al.*, 1981]. *Dziewonski et al.* [1981] independently determined source parameters for five of these earthquakes near the Sunda trench using long-period body wave data recorded on SRO and ASRO instruments. Their focal mechanisms were generally similar to those of Fitch et al. but have a fairly steep north dipping plane and a very shallow south dipping plane. *Dziewonski et al.* [1981] also found a normal-faulting solution for the event of September 23 at 0557, consistent with the first-motion solution of Fitch et al. but inconsistent with the conditioned Rayleigh solution of Fitch et al., as shown in Figure 6*a*.

In the present study a focal mechanism is given for the Sumba main shock based on *P* wave first-motion data (Figures 6*a* and 7 and Table 1). Also, a focal mechanism was determined for the M_S 6.6, normal faulting earthquake that occurred nearly 200 km east of the main shock on April 10, 1978 (Figures 6*b* and 7 and Table 1). This focal mechanism is well-constrained and is very similar to that of the main shock. The main shock focal mechanism is similar to that of *Given and Kanamori* [1980] based on the inversion of surface wave data. The dips of the two planes of the main shock focal mechanism are intermediate between those for Sunda trench aftershocks as determined by *Fitch et al.* [1981] and *Dziewonski et al.* [1981]. This implies that the true focal mechanisms for the Sunda trench aftershocks may be similar to these main shock focal mechanisms, characterized by nearly horizontal T axes. The vertical section of relocated aftershock hypocenters (Figure 5) is consistent with main shock faulting on a steeply dipping plane. Generally, the causative fault of trench earthquakes in other regions is chosen to dip in the direction of motion of the oceanic plate [*Chapple and Forsyth*, 1979], and thus the north dipping fault plane is the most likely for the Sumba main shock rupture and the nearby aftershocks.

By far the greatest number of aftershocks in the trench zone occurred 65–115 km east of the main shock. This activity was concentrated in two segments, one segment at the Sunda trench and the other parallel to it and 25–40 km to the north (Figures 2 and 6*a*). Focal mechanisms in these two segments indicate similar normal-faulting deformation, schematically indicated by 45°N dipping lines through the vertical projections of these two segments (Figure 5).

For the secondary aftershock zone, *Fitch et al.* [1981] and *Dziewonski et al.* [1981] each determined focal mechanisms for the same six earthquakes, and these results indicate that the earthquakes occurred on vertical, right-lateral, strike-slip faults, with *P* axes downdip. In the present study, focal mechanisms were determined for three additional earthquakes in the

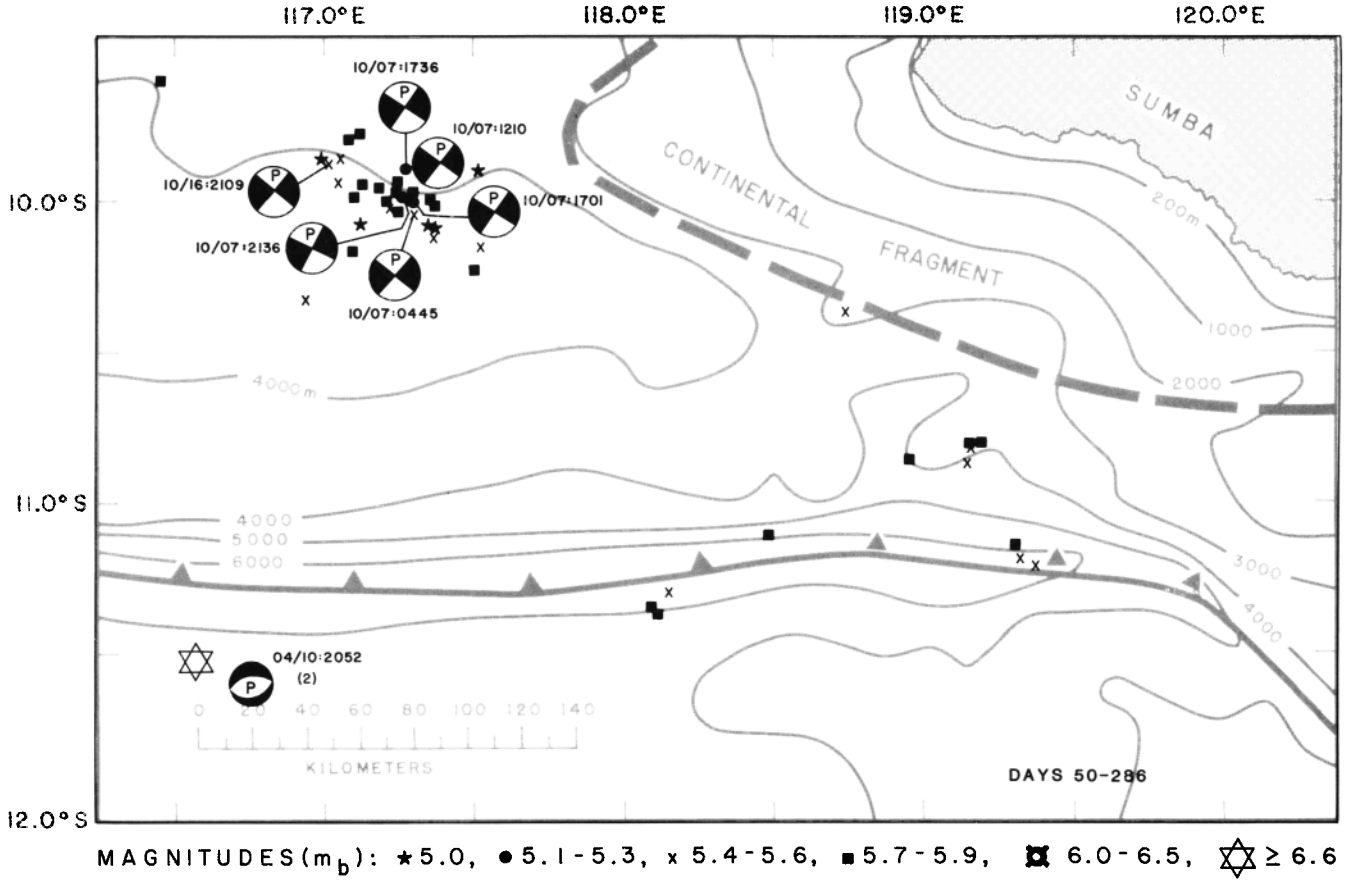

Fig. 6*b*

secondary aftershock zone (Figures 6*a* and 7 and Table 1). These earthquakes occurred several weeks prior to the most active period of this zone, and two of them were located well to the east of the lineation of epicenters. These three earthquakes also have focal mechanisms indicating nearly vertical, strike-slip faulting, but in this case with T axes nearly horizontal and parallel to the dip direction of the subducted plate and with P axes directed southwest.

A focal mechanism solution also was determined for a large (M_S 6.8), shallow earthquake north of Timor, in the South Banda basin (Figures 1*b* and 7 and Table 1). This earthquake, occurring only 8 days after the Sumba main shock, was at a geologically inferred location of back arc thrusting [*Hamilton*, 1979; *Silver et al.*, 1983]. The focal mechanism shows a steep, south dipping thrust plane, striking parallel to the trend of the back arc thrusting (Figures 1*b* and 7) and is the first seismological evidence for back arc thrusting in the South Banda basin. This mechanism is similar to that found for the m_b 5.8 Flores Basin earthquake of December 23, 1978 [*McCaffrey and Nabelek*, 1984*a*], and together these mechanisms support the hypothesis that the collision of Australian continental lithosphere with the Sunda-Banda arc provides conditions for thrusting from the north.

Displacement and Stress Drop

The distribution of aftershocks may indicate that the main shock rupture was about 200 km long and extended deeply into the brittle portion of the oceanic lithosphere. This rupture extended from the seafloor ($h \simeq 6$ km), judging from the generation of a large tsunami, to a depth of about 28 km beneath the seafloor, based on recomputed aftershock depths. Assuming that the main shock rupture occurred on a 45°N dipping fault plane and taking shear modulus $\mu_2 = 4.0 \times 10^{11}$ dyn/cm^2, fault length $L = 200$ km, and fault width $W = 25\ (2)^{1/2}$ km, the average displacement is $\langle u \rangle = M_T(0)/\mu LW = 9$ m, and the average stress drop is $\langle \sigma \rangle = 8\mu\langle u \rangle/\pi W = 26$ MPa (260 bars).

These estimates of stress drop and displacement will require modification if the main shock rupture was less than 100 km long [*Lynnes et al.*, 1985] or if the main shock ruptured as deep as 80–90 km [*Given and Kanamori*, 1980; *Zhang and Kanamori*, 1985]. The latter vertical extent of rupture would indicate an exceptionally deep neutral bending surface or require faulting on both sides of the neutral bending surface. If the main shock rupture involved bending and the bridging of the neutral surface, one might expect thrust-faulting aftershocks deeper than 35–40 km, but such events have not been observed here. *Silver and Jordan* [1983] and *Lynnes et al.* [1985] determined that the moment release and stress drop were concentrated at the upper, more brittle part of the lithosphere, consistent with the finding here that the deepest aftershocks are normal-faulting events about 28 km beneath the top of the lithosphere.

Interpretation: Slab Pull and the 1977 Sumba Earthquake Series

The occurrence of the Sumba earthquake shows that local tension exceeds the compression arising from the northward motion of the Australia-India plate. What is the origin of this tension? The recent cessation of subduction of Australian continental lithosphere [*Bowin et al.*, 1980; *Johnston and Bowin*, 1981] implies that the plate motion rate near the Sumba

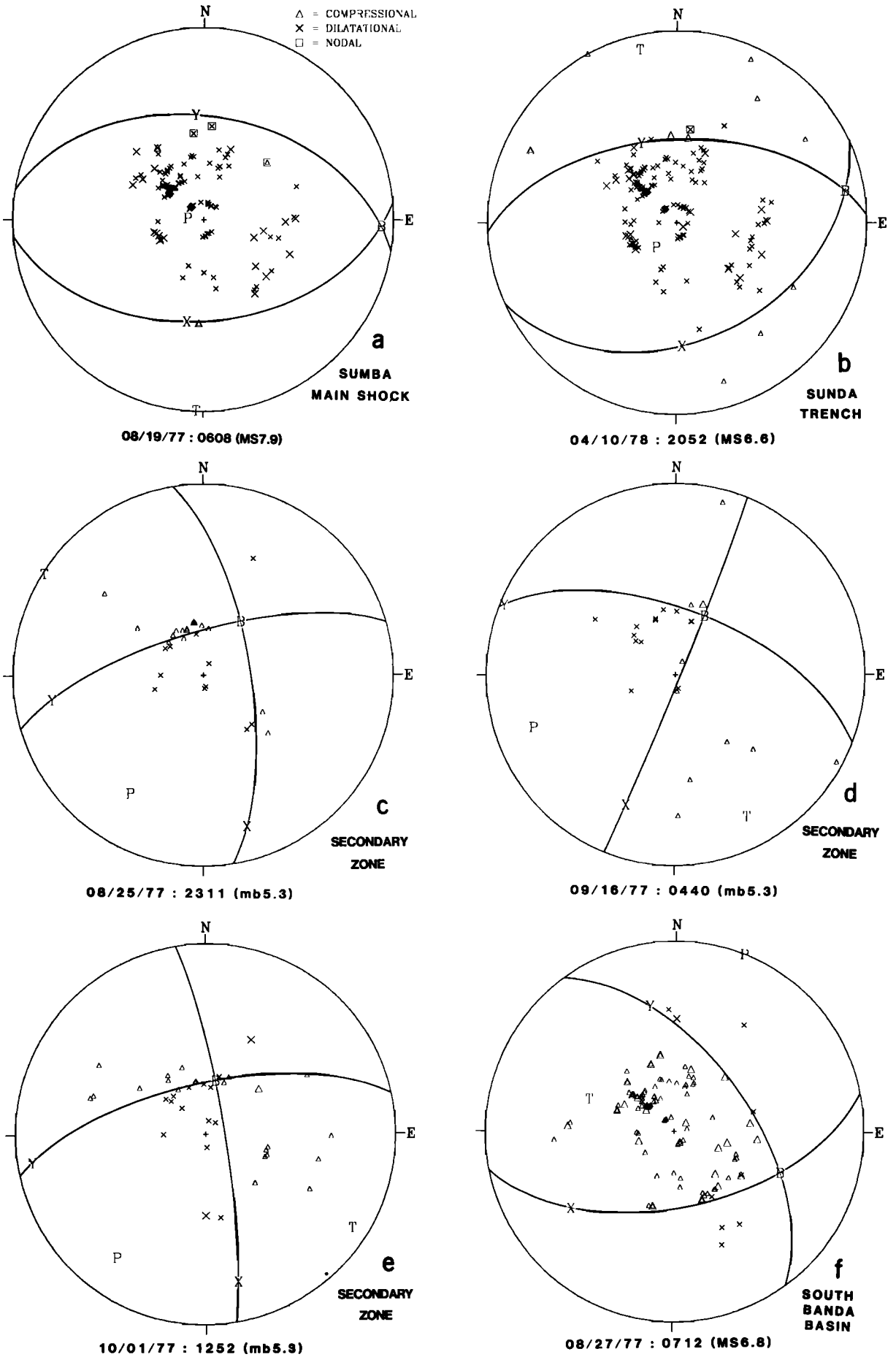
N
△ = COMPRESSIONAL
× = DILATATIONAL
□ = NODAL
E
a
SUMBA
MAIN SHOCK
08/19/77 : 0608 (MS7.9)
b
SUNDA
TRENCH
04/10/78 : 2052 (MS6.6)
c
SECONDARY
ZONE
08/25/77 : 2311 (mb5.3)
d
SECONDARY
ZONE
09/16/77 : 0440 (mb5.3)
e
SECONDARY
ZONE
10/01/77 : 1252 (mb5.3)
f
SOUTH
BANDA
BASIN
08/27/77 : 0712 (MS6.8)

TABLE 1. Source Parameter Data for Earthquakes Shown in Figure 5

Date	Time, UT	Magnitude M_S	Magnitude m_b	Location	Nodal Planes 1 St	1 Dp	1 Sl	2 St	2 Dp	2 Sl	Stress Axes P Tr	P Pl	T Tr	T Pl
Aug. 19, 1977	0608	8.3		Sunda trench	85	46	−100	279	45	−80	276	83	182	1
April 10, 1978	2052	6.6		Sunda pre-trench rise	65	38	−108	267	54	−76	222	76	347	8
Aug. 25, 1977	2311		5.3	secondary zone	351	70	−160	254	71	−21	212	28	303	1
Sept. 16, 1977	0440		5.3	secondary zone	22	88	−152	291	62	−2	250	21	153	18
Oct. 1, 1977	1252		5.3	secondary zone	351	82	−158	258	68	−9	216	21	123	9
Aug. 27, 1977	0712	6.8		South Banda basin	78	57	40	323	57	140	21	0	290	50

St, Strike, Dp, dip, and Sl, slip, are given in degrees for each nodal plane. Strike is measured clockwise from north, dip is measured clockwise from horizontal while looking in direction of strike, and slip is measured in the plane of the fault and positive downward for the hanging wall. Tr, trend, and Pl, plunge, are given in degrees for the axes of greatest and least compressive stress.

earthquake is too low to account for high strains of this earthquake by the continuous bending model of *Hanks* [1979].

At the central section of the Sunda-Banda arc, seismicity exists to depths of about 650 km in the subducted Indian-Australian plate [*Rothé*, 1969; *Cardwell and Isacks*, 1978; *Hamilton*, 1979]. Taking 148 m.y. as the age of oceanic lithosphere at the site of the Sumba earthquake [*Hamilton*, 1979] indicates a total lithospheric thickness of about 100 km [*Anderson and Minster*, 1980]. Slab pull forces are proportional to the excess mass of subducted lithosphere. Given the great age, thickness, and depth of the subducted oceanic lithosphere at the eastern Sunda arc, the slab pull force downdip of the Sumba earthquake must be close to the maximum that exists globally. The absolute magnitude of the slab pull force that is transmitted through subduction zones must be large as the works by *Isacks and Molnar* [1971], *Smith and Toksöz* [1972], *Forsyth and Uyeda* [1975], *Solomon et al.* [1975], *Richter* [1977], *Chapple and Tullis* [1977], and *Carlson* [1983] clearly indicate that the negative buoyancy of subducted oceanic lithosphere (slab pull) is the major driving force for plate motions. Thus it is apparent that very large slab pull forces can be transmitted through the shallow subduction zone in the region of the Sumba earthquakes.

A partial decoupling of the interface thrust zone (in the sense of *Kanamori* [1971, 1977], *Uyeda and Kanamori* [1979], and *Ruff and Kanamori* [1980]) by the slab pull force may explain the absence of great interface thrust earthquakes at the eastern Sunda arc. Also, the recent cessation of subduction of adjacent continental lithosphere may lead to local uplift of the overriding plate and contribute to a partial decoupling of the interface thrust zone. Such decoupling allows much of the local slab pull force to be transmitted updip to the zone of plate bending beneath the trench. Because the slab pull force greatly exceeds the ridge push force and because the subduction rate is low at the Sumba earthquake zone, large, local slab pull forces are inferred to cause large bending stresses. The 1977 Sumba earthquake is interpreted to be caused by these bending stresses of slab pull origin.

Stresses originating with slab pull forces would be concentrated beneath the trench because of the prior bending there [*McKenzie*, 1969], and the Sumba earthquake may represent a reactivation of a major normal fault beneath the trench. The subhorizontal T axes for the main shock and other trench earthquakes and the subhorizontal T axes for the three early aftershocks in the secondary zone are consistent with this interpretation for the origin of the Sumba earthquake (Figure 6*a*). Taking slab pull forces to have caused the Sumba main shock, the 9-m displacement on a 45°N dipping fault could be achieved by about 7.5 m of extension within and parallel to the shallow descending plate, as shown in Figure 8.

Other regional evidence for the effects of the slab pull force are the 1963, magnitude 7.8 earthquake occurring at 130°E at 100 km depth [*Osada and Abe*, 1981] and smaller, intermediate-depth earthquakes near western Timor [*McCaffrey et al.*, 1985], all of which have vertical tension axes.

The location of the secondary zone of aftershocks within the oceanic lithosphere eliminates these aftershocks caused by a rebound of the overriding plate, as was observed following the 1965 Rat Island earthquake [*Stauder*, 1968; *Spence*, 1977]. Although the collision of Australia with the Banda arc produces shallow compression east of the Sumba earthquake, effects of such compression within the subducted plate may be overridden by the tensional (slab pull) forces that caused the Sumba earthquake.

If slab pull is the primary cause of plate motions, then it follows that slab pull is a primary determiner of subduction rates. However, because the subduction of Australian continental lithosphere has slowed to nearly zero, it is inferred that this lithosphere provides a very stong resistance to any motions caused by slab pull forces. The magnitudes of slab pull forces from the central Sunda arc through the central Banda arc may be comparable [*Cloetingh and Wortel*, 1985], and the differences in subduction rates are due to differences in shallow resistance to subduction. Thus the observation that the subduction rate is more rapid west of the Sumba earthquakes

Fig. 7. (opposite) P wave first-motion data for the six new focal mechanism solutions done in this study, plotted on stereographic projections of the lower focal hemisphere. Small symbols represent short-period data (largely from ISC catalog) and large symbols represent long-period data (read for this study from WWSSN, SRO, and ASRO stations). Fitted nodal planes are shown with the poles of the x and y planes and the pressure P, tensional T, and null B axes.

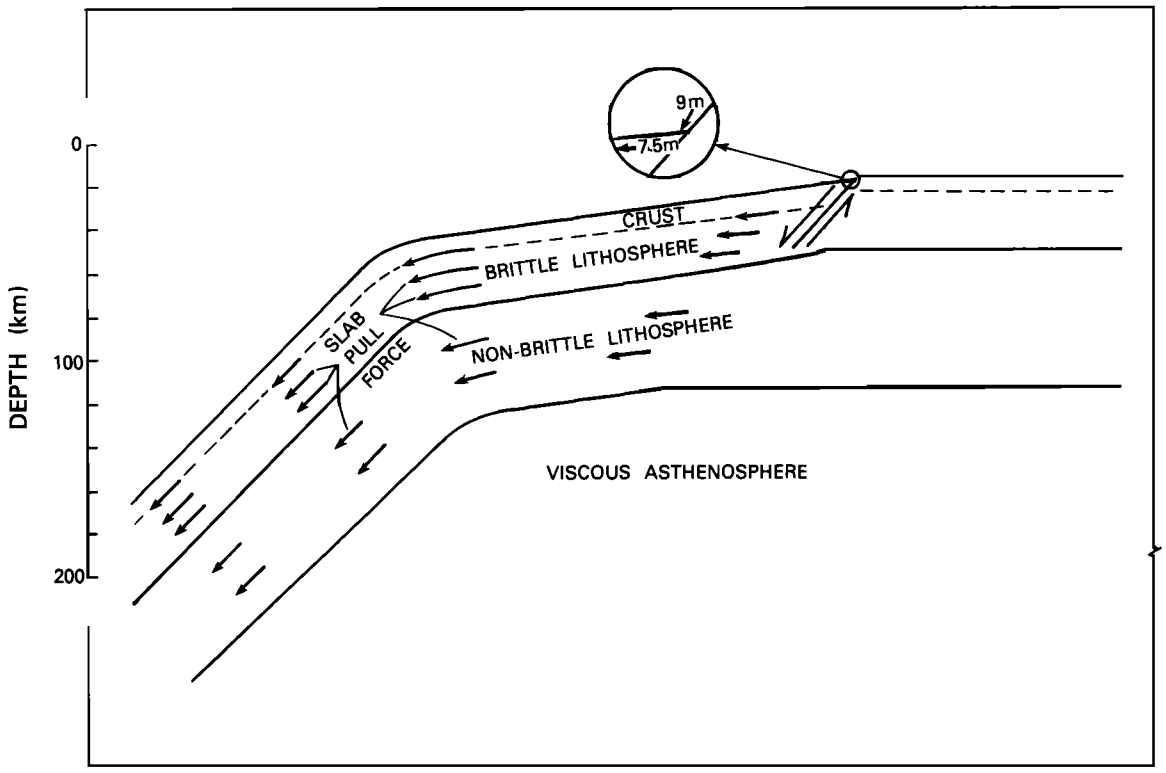

Fig. 8. Schematic cross section of subducted lithosphere, indicating the main shock displacement and the causative, slab pull forces.

than east of them does not imply that the magnitude of the slab pull force changes much across this zone. The right-lateral displacement observed for the secondary zone of aftershocks primarily is due to this differential subduction rate (Figure 9).

Also, the secondary zone is close to the west side of the Sumba continental fragment [*Hamilton*, 1979; *Chamalaun et al.*, 1982]. There may be some interaction between the subducted plate and the root of the Sumba continental fragment as indicated by the localization beneath Sumba of moderate-sized, thrust-faulting earthquakes [*Cardwell and Isacks*, 1978; *McCaffrey and Nabelek*, 1984*b*]. This interaction may cause further resistance to subduction and augment the right-lateral, strike-slip displacement within the oceanic plate to the west of Sumba.

In the model developed here, subducted lithosphere extended by slab pull forces primarily is supported at the eastern Sunda trench. Steadily increasing tensional stresses of slab pull origin led to the main shock. After the main shock, in this model, a downdip propagating, Maxwellian strain pulse returned the plate to a less extended state. The release of the slab-pulled plate at its fixed end (by the main shock) is analogous to the release of one end of a stretched, damped spring with the spring then moving toward its unstretched shape.

The focal mechanisms for aftershocks that occurred in the secondary zone after day 50 show downdip *P* axes (Figure 6*b*). This may be caused as the suddenly released free end of the stretched plate overshoots the plate's equilibrium position, leading to a downdip propagating pulse of compression strain. A more likely explanation for the downdip *P* axes is that the rapidly moving pulse of downdip plate motion is resisted by the overriding plate, causing localized compression in the upper part of the subducting plate. The timing of the triggered aftershocks corresponds to the downdip velocity of the Maxwellian strain pulse, governed by the viscosity of the lower bounding mantle and the elastic properties of the overriding accretionary wedge and the subducting plate. Similar downdip strain pulses following decoupling earthquakes may also explain the downdip *P* axes of large, anomalous earthquakes in the upper mantle that followed the decoupling earthquakes of 1965, Rat I. [*Spence*, 1977] and 1960, Chile [*Astiz and Kanamori*, 1985].

DISCUSSION

Is it coincidence that the main shock location is directly along the strike of the secondary aftershock zone? While it would be difficult to relate the secondary zone to the main shock by compression from the oceanic side, one may argue that slab pull forces produced right-lateral deformation in a preexisting zone of weakness at the location of the secondary aftershock lineation (near the west side of the Sumba continental fragment). The resulting extension could migrate updip, ultimately initiating tensional failure at the main shock hypocenter.

The downdip movement of a 100-km-thick plate over the days and weeks following the main shock could have moment contributions far in excess of the seismic moment for the main shock which was computed using only the initial 1000 s of surface wave energy. If the moment of this motion of subducted oceanic lithosphere is much greater than the seismic moment of the main shock, the corresponding global displacement field could provide an excitation pulse for the Chandler wobble, as possibly observed for the Sumba earthquake by *Gross and Chao* [1985].

The same set of forces that cause plate motions may also cause plate bending; that is, the cause of plate bending may be

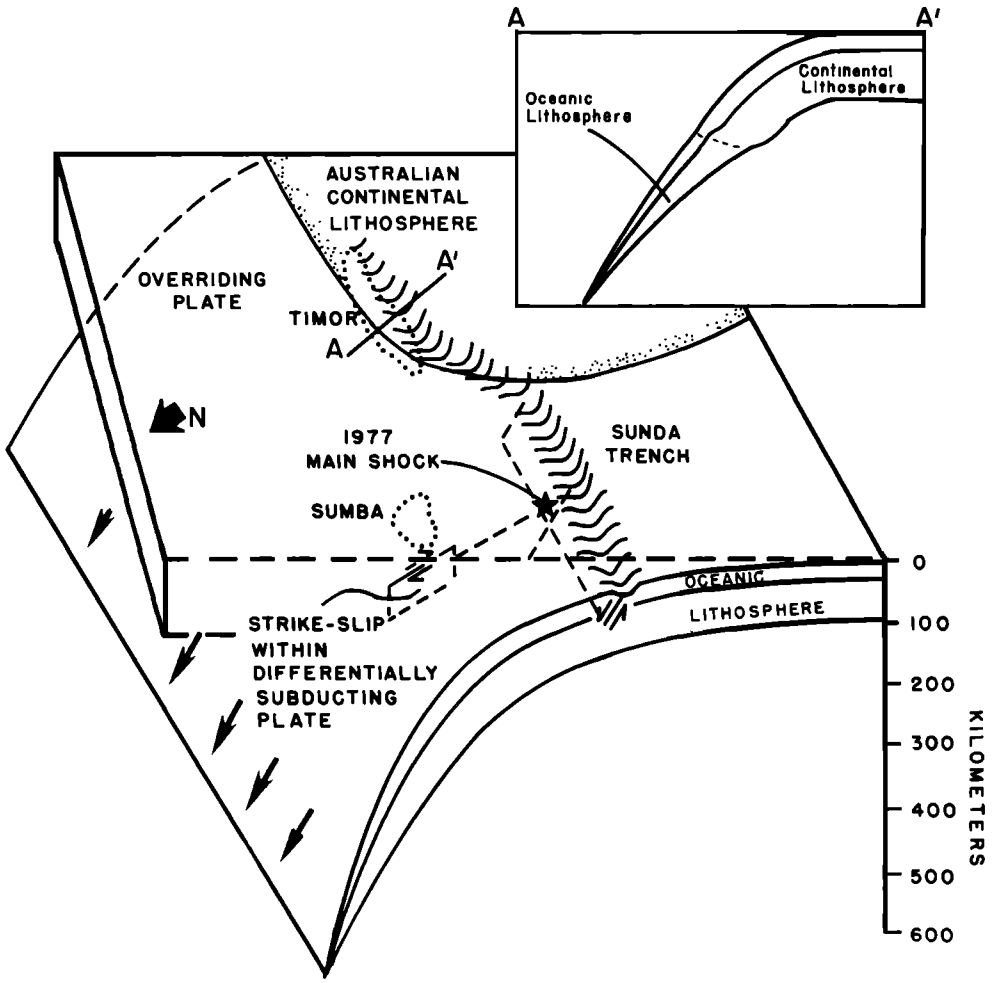

Fig. 9. Perspective diagram of the region of the 1977 Sumba earthquake. Subduction of Australian continental lithosphere (inset) has slowed to near zero, whereas the subduction of oceanic lithosphere west of the Sumba main shock is continuing. Slab pull forces are comparable for both zones.

dominated by the slab pull force. Typically, the slab pull force will be blocked by the locked interface thrust zone. However, after a great, interface thrust earthquake the slab pull force can propagate trenchward, sometimes producing normal-faulting earthquakes near the trench [*Stauder*, 1968; *Spence*, 1977; *Chapple and Forsyth*, 1979; *Hanks*, 1979; *Imoto*, 1981]. This episodic loading of a bending moment at the trench and outer rise system may be sufficient to sustain the geometry of these features.

Conclusions

The unique tectonic setting of the Sumba earthquake helps to isolate the slab pull force as the cause of the 1977 Sumba earthquake series and as an important cause of plate bending at the eastern Sunda trench. A careful analysis of depths and focal mechanism data of the Sumba aftershocks shows that the deepest trench events are consistent with normal faulting to a depth of 28 km into the lithosphere. No evidence exists here for thrust faulting, which would help establish the depth of the neutral bending surface.

In the shallow-acting slab pull model, slab pull forces stretched the downdip oceanic lithosphere prior to the main shock. The locally large slab pull force has largely decoupled the interface thrust zone. This allows tensional stresses due to the slab pull force to exist updip from the decoupled interface zone, leading to the normal-faulting earthquakes of the Sumba earthquake series. Following the main shock, a downdip propagating strain pulse returned the subducted plate to a less extended state and triggered late aftershocks within the subducted plate.

Acknowledgments. Don Forsyth, Carl Bowin, and an anonymous Associate Editor gave provocative and helpful reviews. I thank Stu Nishenko, Warren Hamilton, and Jim Dewey for their critical comments on an earlier draft of this paper. Jim Dewey helped me with the JHD recomputations of hypocenters, George Choy introduced me to broadband digital seismic data, and Russ Needham and Madeleine Zirbes helped in determining the new focal mechanism solutions. This research was partially funded by the U.S. Agency for International Development agreement BOF-0000-P-IC-4051-00.

References

Anderson, D. L., and J. B. Minster, Seismic velocity, attenuation and rheology of the upper mantle, *U.S. Geol. Surv., Open File Rep. 80-625*, 952-967, 1980.

Astiz, L., and H. Kanamori, Interplate coupling and stress variation within the subducted slab at intermediate depth associated with the great 1960 Chile earthquake, *Eos Trans. AGU*, *66*, 957, 1985.

Bowin, C., G. M. Purdy, C. Johnston, G. G. Shor, L. Lawver, H. M. S. Hartano, and P. Jezek, Arc-continent collision in the Banda Sea region, *Am. Assoc. Pet. Geol. Bull.*, *64*, 868-915, 1980.

Caldwell, J. G., W. F. Haxby, D. E. Karig, and D. L. Turcotte, On the applicability of a universal elastic trench profile, *Earth Planet. Sci. Lett.*, *31*, 239-246, 1976

Cardwell, R. K., and B. L. Isacks, Geometry of the subducted lithosphere beneath the Banda Sea in eastern Indonesia from seismicity and fault plane solutions, *J. Geophys. Res.*, *83*, 2825–2838, 1978.

Carlson, R. L., Plate motions, boundary forces, and horizontal temperature gradients: Implications for the driving mechanism, *Tectonophysics*, *99*, 149–164, 1983.

Chamalaun, F. H., and A. E. Grady, The tectonic model for Timor: A new model and its implications for petroleum exploration, *APEA J.*, *18*, 102–108, 1978.

Chamalaun, F. H., A. E. Grady, C. C. von der Boch, and H. M. S. Hartano, Banda arc tectonics: The significance of Sumba Island (Indonesia), Studies in Continental Margin Geology, edited by J. S. Watkins and C. L. Drake, *Mem. Am. Assoc. Pet. Geol.*, *34*, 361–375, 1982.

Chapple, W. M., and D. W. Forsyth, Earthquakes and bending of plates at trenches, *J. Geophys. Res.*, *84*, 6729–6749, 1979.

Chapple, W. M., and T. E. Tullis, Evaluation of the forces that drive the plates, *J. Geophys. Res.*, *82*, 1967–1984, 1977.

Christensen, D., and L. Ruff, Outer-rise earthquakes and seismic coupling, *Geophys. Res. Lett.*, *10*, 697–700, 1983.

Christensen, D., and L. Ruff, The rupture process of the 1985 Chile earthquake, *Eos Trans. AGU*, *66*, 951, 1985.

Cloetingh, S., and R. Wortel, Regional stress field of the Indian plate, *Geophys. Res. Lett.*, *12*, 77–80, 1985.

Curray, J. R., G. G. Shor, Jr., R. W. Raitt, and M. Henry, Seismic refraction and reflection studies of crustal structure of the eastern Sunda and western Banda arcs, *J. Geophys. Res.*, *82*, 2479–2489, 1977.

Dewey, J. W., Seismicity studies with the method of joint hypocenter determination, Ph.D. dissertation, Univ. of Calif., Berkeley, 1971.

Dewey, J. W., and W. Spence, Seismic gaps and source zones of recent large earthquakes in coastal Peru, *Pure Appl. Geophys.*, *117*, 1148–1171, 1979.

Dziewonski, A. M., T.-A. Chou, and J. H. Woodhouse, Determination of earthquake source parameters from waveform data for studies of global and regional seismicity, *J. Geophys. Res.*, *86*, 2825–2852, 1981.

Fitch, T. J., Earthquake mechanisms and island arc tectonics in the Indonesian-Philippine region, *Bull. Seismol. Soc. Am.*, *60*, 565–591, 1970.

Fitch, T. J., Plate convergence, transcurrent faults, and internal deformation adjacent to southeast Asia and the western Pacific, *J. Geophys. Res.*, *77*, 4432–4460, 1972.

Fitch, T. J., and P. Molnar, Focal mechanisms along inclined earthquake zones in the Indonesia-Philippine region, *J. Geophys. Res.*, *75*, 1431–1444, 1970.

Fitch, T. J., R. G. North, and M. W. Shields, Focal depths and moment tensor representations of shallow earthquakes associated with the great Sumba earthquake, *J. Geophys. Res.*, *86*, 9357–9374, 1981.

Forsyth, D. W., Determinations of focal depths of earthquakes associated with the bending of oceanic plates at trenches, *Phys. Earth Planet. Inter.*, *28*, 141–160, 1982.

Forsyth, D., and S. Uyeda, On the relative importance of driving forces of plate motion, *Geophys. J. R. Astron. Soc.*, *43*, 163–200, 1975.

Given, J. W., and H. Kanamori, The depth extent of the 1977 Sumbawa, Indonesia earthquake, *Eos Trans. AGU*, *61*, 1044, 1980.

Gross, R. H., and B. F. Chao, Excitation study of the LAGEOS-derived Chandler wobble, *J. Geophys. Res.*, *90*, 9369–9380, 1985.

Hamilton, W., Tectonics of the Indonesian region, *U.S. Geol. Surv. Prof. Pap. 1078*, 1979.

Hanks, T., The Kuril Trench–Hokkaido rise system: Large shallow earthquakes and simple models of deformation, *Geophys. J. R. Astron. Soc.*, *23*, 173–189, 1971.

Hanks, T., Deviatoric stresses and earthquake occurence at the outer rise, *J. Geophys. Res.*, *84*, 2343–2368, 1979.

Imoto, M., On migration of aftershocks following large thrust earthquakes in subduction zones, *Rep. 25*, pp. 29–86, Natl. Res. Cent. for Disaster Prev., Sakura-mura, Ibaraki-ken, Japan, 1981.

Isacks, B., and P. Molnar, Distribution of stresses in the descending lithosphere from a global survey of focal mechanisms of mantle earthquakes, *Rev. Geophys.*, *9*, 103–174, 1971.

Johnston, C. R., and C. O. Bowin, Crustal reactions resulting from the mid-Pliocene to recent continental-island arc collision in the Timor region, *BMR J. Aust. Geol. Geophys.*, *6*, 223–243, 1981.

Kanamori, H., Seismological evidence for a lithospheric normal faulting–The Sanriku earthquake of 1933, *Phys. Earth Planet. Inter.*, *4*, 289–300, 1971.

Kanamori, H., Mechanism of tsunami earthquakes, *Phys. Earth Planet. Inter.*, *6*, 346–359, 1972.

Kanamori, H., Seismic and aseismic slip along subduction zones and their tectonic implications, in *Island Arcs, Deep Sea Trenches, and Back-Arc Basins, Maurice Ewing Ser.*, vol. 1, edited by M. Talwani and W. C. Pitman III, pp. 163–174, AGU, Washington, D. C., 1977.

Katili, J. A., Volcanism and plate tectonics in the Indonesian island arcs, *Tectonophysics*, *26*, 165–188, 1975.

Lynnes, C. S., T. Lay, and L. J. Ruff, Rupture process of the 1977 Sumba earthquake, *Eos Trans. AGU*, *66*, 957, 1985.

McAdoo, D. C., J. G. Caldwell, and D. L. Turcotte, On elastic-perfectly plastic bending of the lithosphere under generalized loading with application to the Kuril Trench, *Geophys. J. R. Astron. Soc.*, *51*, 11–26, 1978.

McCaffrey, R., and J. Nabelek, The geometry of backarc thrusting along the eastern Sunda arc, Indonesia: Constraints from earthquake and gravity data, *J. Geophys. Res.*, *89*, 6171–6179, 1984*a*.

McCaffrey, R. and J. Nabelek, Depths and source mechanisms of earthquakes from the eastern Sunda arc, Indonesia, *Eos Trans. AGU*, *65*, 997, 1984*b*.

McCaffrey, R., P. Molnar, S. W. Roecker, and Y. S. Joyodiwiyo, Microearthquake seismicity and fault plane solutions related to arc-continent collision in the eastern Sunda arc, Indonesia, *J. Geophys. Res.*, *90*, 4511–4528, 1985.

McCann, W. R., S. P. Nishenko, L. R. Sykes, and J. Krause, Seismic gaps and plate tectonics: Seismic potential for major boundaries, *Pure Appl. Geophys.*, *117*, 1082–1147, 1979.

McKenzie, D. P., Speculations on the consequences and causes of plate motions, *Geophys. J. R. Astron. Soc.*, *18*, 1–32, 1969.

Mogi, K., Relationship between shallow and deep seismicity in the western Pacific region, *Tectonophysics*, *17*, 1–22, 1973.

Molnar, P., and D. Gray, Subduction of continental lithosphere: Some constraints and uncertainties, *Geology*, *7*, 58–62, 1979.

National Earthquake Information Service, Preliminary determination of epicenters, monthly listing, August 1977, U.S. Geol. Surv., Reston, Va., 1977.

Nishenko, S., Seismic potential for large and great interplate earthquakes along the Chilean and southern Peruvian margins of South America: A quantitative reappraisal, *J. Geophys. Res.*, *90*, 3589–3615, 1985.

Osada, M., and K. Abe, Mechanism and tectonic implications of the great Banda Sea earthquake of November 4, 1963, *Phys. Earth Planet. Inter.*, *25*, 129–139, 1981.

Parsons, B., and P. Molnar, The origin of outer topographic rises associated with trenches, *Geophys. J. R. Astron. Soc.*, *45*, 707–712, 1976.

Pennington, W. D., The effect of oceanic crustal structure on phase changes and subduction, *Tectonophysics*, *102*, 377–398, 1984.

Richter, F. M., On the driving mechanism of plate tectonics, *Tectonophysics*, *38*, 61–88, 1977.

Roecker, S. W., Velocity structure of the Pamir–Hindu Kush region: Possible evidence of subducted crust, *J. Geophys. Res.*, *87*, 945–959, 1982.

Rothé, J. P., *The Seismicity of the Earth*, UNESCO, Paris, 1969.

Ruff, L., and H. Kanamori, Seismicity and the subduction process, *Phys. Earth Planet. Inter.*, *23*, 240–252, 1980.

Silver, E. A., W. Reed, R. McCaffrey, and Y. Joyodiwiryo, Back arc thrusting in the eastern Sunda arc, Indonesia: A consequence of arc-continent collision, *J. Geophys. Res.*, *88*, 7429–7448, 1983.

Silver, P. G., and T. H. Jordan, Total-moment spectra of fourteen large earthquakes, *J. Geophys. Res.*, *88*, 3273–3293, 1983.

Simkin, T., L. Siebert, L. McClellend, D. Bridge, C. Newhall, and J. H. Latter, *Volcanoes of the World*, 232 pp., Hutchinson Ross, Stroudsburg, Pa., 1981.

Smith, A. T., and M. N. Toksöz, Stress distribution beneath island arcs, *Geophys. J. R. Astron. Soc.*, *29*, 289–318, 1972.

Solomon, S. C., N. H. Sleep, and R. M. Richardson, On the forces driving plate tectonics: Inferences from absolute plate velocities and intraplate stress, *Geophys. J. R. Astron. Soc.*, *42*, 769–801, 1975.

Spence, W., The Aleutian arc: Tectonic blocks, episodic subduction, strain diffusion, and magma generation, *J. Geophys. Res.*, *82*, 213–230, 1977.

Stagg, H. M. J., The geology and evolution of the Scott Plateau, *APEA J.*, *18*, 34–43, 1978.

Stauder, W., Tensional character of earthquake foci beneath the Aleu-

tian trench with relation to seafloor spreading, *J. Geophys. Res.*, *73*, 7693–7701, 1968.

Uyeda, S., and H. Kanamori, Back arc opening and the mode of subduction, *J. Geophys. Res.*, *84*, 1049–1061, 1979.

Vogt, P. R., N. Z. Cherkis, and G. A. Morgan, Project Investigator, I, Evolution of the Australia-Antarctic discordance deduced from a detailed aeromagnetic study, in *Proceeding 4th International Symposium on Antarctic Earth Science*, edited by R. L. Oliver, P. R. James, and J. B. Jago, pp. 608–613, Australian Academy of Science, Canberra, 1983.

Ward, S. N., Body-wave inversion: Moment tensors and depths of oceanic intraplate bending earthquakes, *J. Geophys. Res.*, *88*, 9315–9330, 1983.

Watts, A. B., J. H. Bodine, and M. S. Steckler, Observations of flexure and the state of stress in the oceanic lithosphere, *J. Geophys. Res.*, *85*, 6369–6376, 1980.

Weissel, J. K., and D. E. Hayes, The Australian-Antarctic discordance: New results and implications, *J. Geophys. Res.*, *79*, 2579–2587, 1974.

Zhang, J., and H. Kanamori, Determination of vertical extent of faulting of large earthquakes using long-period surface waves, *Eos Trans. AGU*, *66*, 963, 1985.

W. Spence, U.S. Geological Survey, National Earthquake Information Center, Box 25046, MS 967, Denver, CO 80225.

(Received January 23, 1985;
revised March 24, 1986;
accepted March 24, 1986.)